

**Maximizing the Symbiosis of Static and Dynamic Bonds in  
Self-Healing Boronic Ester Networks**

Journal:	<i>Polymer Chemistry</i>
Manuscript ID	PY-ART-01-2018-000123.R1
Article Type:	Paper
Date Submitted by the Author:	12-Mar-2018
Complete List of Authors:	Cash, Jessica; University of Florida, Department of Chemistry Kubo, Tomohiro; University of Florida, Department of Chemistry Dobbins, Daniel; University of Florida, Department of Chemistry Sumerlin, Brent; University of Florida, Department of Chemistry;

# Maximizing the Symbiosis of Static and Dynamic Bonds in Self-Healing Boronic Ester Networks

Jessica J. Cash, Tomohiro Kubo, Daniel J. Dobbins, Brent S. Sumerlin\*

George & Josephine Butler Polymer Research Laboratory, Center for Macromolecular Science & Engineering, Department of Chemistry, University of Florida, Gainesville, FL 32611, USA  
E-Mail: [sumerlin@chem.ufl.edu](mailto:sumerlin@chem.ufl.edu)

## Abstract

Networks that contain boronic ester crosslinks undergo dynamic bond exchange that enables self-healing behavior and reprocessing. However, networks crosslinked exclusively by rapidly exchanging bonds are also susceptible to creep and stress relaxation, which limits many potential materials applications. In this report, we studied the effect of combining various ratios of dynamic boronic ester crosslinks and static (i.e., irreversible) crosslinks in bulk polymeric materials. We also considered different mechanisms of bond exchange by preparing networks that contained free diols to enable crosslink exchange of boronic esters by transesterification. The networks were evaluated in terms of responsiveness to moisture, proclivity towards deformation, and ability to self-heal. The networks containing free diols could be remolded and healed upon heating. By controlling the humidity and temperature of the environment, the dominant boronic ester exchange mechanism could be shifted from hydrolysis/re-esterification to transesterification. Incorporating a fraction of permanent crosslinks yielded networks that maintained their structural integrity yet still underwent good healing and reproducible repair after multiple cut/heal cycles. When both free diols and irreversible crosslinks were incorporated into a single network, shape stability was enhanced, and improved healing was observed when compared to networks that contained either free diol or permanent crosslinks independently.

## Introduction

When designing polymeric materials capable of both long-term durability and end-of-life recycling, having the capacity to tune macroscopic structure as well as mechanical properties is critical. The stability of the initial macroscopic shape of most polymeric materials is partly determined by an ability to relieve internal stresses developed during synthesis.<sup>1</sup> However, stability in materials crosslinked via dynamic bonds can also be established post-synthesis, given sufficient time for crosslink exchange. Materials made from networks with dynamic bonds can function as static or dynamic networks, depending on the rate of crosslink exchange. As a result, selection of the type of dynamic linkage used for crosslinking greatly influences the overall behavior of the resulting material.<sup>2,3</sup> However, it is important to consider that networks containing dynamic linkages do not consist solely of bonds capable of exchange.<sup>4</sup> The majority of the bonds present in these networks are static. These static bonds affect the dynamics of the network by restricting local mobility and dictating the positioning of the reactive moieties after crosslink dissociation.<sup>5</sup>

Tremendous interest has been paid to materials that contain dynamic crosslinks. The reversible nature of the crosslinks allows, in many cases, self-healing and reprocessability. However, dynamic crosslink exchange can also lead to creep and stress relaxation, which prevents the materials from being useful for many applications. Whether the shape of a particular material is persistent or transient is largely determined by the selection, placement, and ratio of static to dynamic bonds present in the network.

Control over crosslink density can be maintained in a dynamic network through careful selection of a crosslink exchange mechanism. Covalent adaptable networks (CANs), defined as reversibly crosslinked polymers with a sufficient density of reversible bonds to allow the

network to respond chemically to an external stimulus,<sup>6</sup> can be divided into two types based on the mechanism of exchange operative within the network.<sup>7</sup> In dissociative CANs, bonds are continuously broken and re-formed. In this case, crosslink density depends on the equilibrium between the associated and dissociated bonds. In associative CANs, bond cleavage is accompanied by simultaneous formation of a new crosslink. As a result, crosslink density remains constant. The dissociative mechanism can produce large local concentrations of reactive functionalities at damaged interfaces, facilitating bridge formation, an important step in the self-healing process.<sup>8</sup> The associative mechanism, in contrast, affords retention of crosslink density and mechanical properties.<sup>9</sup> This latter mechanism has been most often demonstrated in networks that undergo crosslink exchange via traditional thermally-responsive transesterification reactions,<sup>10-12</sup> though several other creative chemistries have been considered recently.<sup>7,13-22</sup> Despite the recent advances in this area, there still exists a need for increased chemical diversity in the field of associative CANs.

While boronic ester and diol transesterification reactions have been investigated and characterized in small molecule contexts,<sup>23,24</sup> this type of chemistry has been less widely applied to polymeric systems. In a recent example of boronic ester transesterification in a polymer network, a diol-functionalized polymer was crosslinked with two types of difunctional boronic esters.<sup>25</sup> Network healing could occur by a combination of two mechanisms: hydrolysis/re-esterification (dissociative exchange) and transesterification (associative exchange). Given the relatively low hydrolytic stability of most boronic esters, a dry environment would be needed to isolate transesterification as the only operative mechanism of bond exchange.<sup>23</sup> Manipulating the contributions of hydrolysis and transesterification could lead to materials that not only exhibit a rapid response to external stimuli but also high crosslink retention, enabling improved

conservation of mechanical properties. The combination of two dynamic exchange mechanisms operating on different timescales for self-healing applications has previously been reported by other authors.<sup>26,27</sup> Boronic esters can potentially achieve similar properties with a single type of crosslink.

Another way molecular structure can be harnessed to control the macroscopic behavior of polymeric networks is through the selective placement of static bonds between crosslinking points to complement and support connections with exchangeable bonds. Permanent crosslinking enables retention of mechanical properties and reduces the ability of the material to relax under an applied stress,<sup>28-30</sup> as has been demonstrated by swelling experiments on gels with various concentrations of permanent crosslinker.<sup>31</sup> By varying the quantity of permanent crosslinks, networks can be designed so that an irreversible framework allows for better macroscopic structural integrity, while a shifting equilibrium exchange in dynamic bonds provides the capacity for healing.

We are interested in directing macromolecular behavior through the design of networks that marry dynamic and static chemistries. We sought to improve the structural properties of self-healing materials through mechanistic control of the exchange reaction and by the inclusion of permanent crosslinks within otherwise reversible networks, expanding upon our previous investigations of reversibly crosslinked polymer architectures in solution, such as stars,<sup>32-36</sup> micelles,<sup>37-40</sup> and gels,<sup>41,42</sup> to explore dynamic networks in the bulk state.<sup>43</sup>

We envisioned that the boronic ester functionality would be well-suited for exploring the effect of network architecture on shape stability and dynamicity in self-healing materials through simultaneous stimuli-responsive associative and dissociative exchange and the incorporation of irreversible crosslinks. We prepared three systems: (Figure 1a) boronic ester networks with

various concentrations of excess diol for concurrent bond exchange via dissociative hydrolysis/re-esterification and associative transesterification, (Figure 1b) boronic ester networks that were augmented by the addition of irreversible crosslinks, and (Figure 1c) boronic networks that contained both free diols and irreversible crosslinks. For each system, water absorption, stress-relaxation, and healing behaviors were characterized to elucidate the relative roles of static and dynamic crosslinks. While the initial two systems excelled at rearrangement and shape retention, respectively, the third system yielded a material that favorably balanced both behaviors.

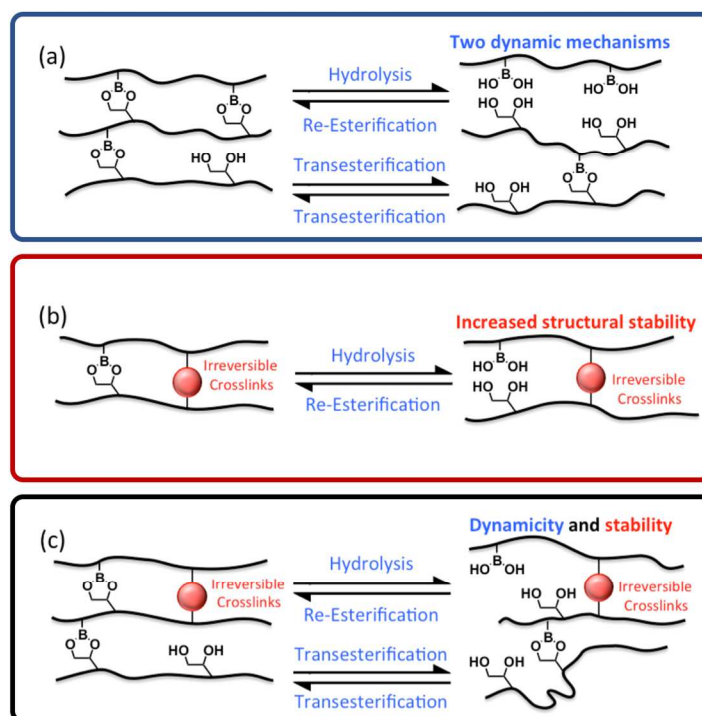


**Figure 1.** (a) Boronic ester networks with excess diol, (b) boronic ester networks that incorporate irreversible crosslinks, and (c) boronic ester networks that include excess diol and irreversible crosslinks.

## Experimental

**Materials.** 4-((Allyloxy)methyl)-2-(4-vinylphenyl)-1,3,2-dioxaborolane (VPBE) was prepared as previously reported,<sup>43</sup> except the purification was modified to eliminate the need for centrifugation. Dimethylsulfoxide-*d*<sub>6</sub> (*d*-DMSO, Cambridge Isotopes, 99.9% D) was dried overnight over 4 Å molecular sieves. Dichloromethane (DCM, Sigma-Aldrich) was dried using an anhydrous solvent system (Innovative Technologies). 4-Vinylphenylboronic acid (VPBA, Combi-Blocks, 98%), 3-allyloxy-1,2-propanediol (APD, Acros Organics, 98%), pentaerythritol tetrakis(3-mercaptopropionate) (PTMP, Sigma-Aldrich, 95%), 3,6-dioxa-1,8-octanedithiol (DODT, TCI America, 95%), 2,2-dimethoxy-2-phenylacetophenone (DMPA, Sigma-Aldrich, 99%), potassium chloride (BDH, 99%), potassium acetate (Macron Chemicals, 99%), tri(ethylene glycol) divinyl ether (TEGDVE, Sigma-Aldrich, 98%), and molecular sieves (4 Å, Mallinckrodt) were used as received.

**Instrumentation and Analysis.** Infrared spectra were collected on a Perkin Elmer Spectrum One FTIR spectrometer equipped with a ZnSe crystal attenuated total reflectance (ATR) accessory. Differential scanning calorimetry (DSC) measurements were performed on a TA Instruments Q1000 equipped with a liquid nitrogen cooling accessory and calibrated using sapphire and high purity indium metal. All samples were prepared in hermetically sealed pans (4–7 mg/sample) and were referenced to an empty pan. A scan rate of 10 °C per min and helium purge gas were used. Glass transition temperatures were evaluated as the midpoint of a step change in heat capacity. DSC experiments were conducted as follows: samples pre-conditioned

in desiccators were heated to 50 °C, followed by cooling at 10 °C per min to -80 °C, and then heated to 50 °C at 10 °C per min. Data reported reflects the average of the second and third heating scans. Tensile tests and stress relaxation tests were performed on a TA.XTPlus texture analyzer from Texture Technologies with a 5 kg load cell using test specimens in the form of dogbones that were sized according to ASTM standard D1708 with a 15 mm grip-to-grip separation at 25°C and 50% humidity. The tensile data reported are the average of five measurements collected with a rate of 10 mm/min. For the stress relaxation experiments, all network compositions were equilibrated for a minimum of 24 h in either a desiccator, to approximate 0% humidity, or the desired salt humidity chamber (*vide infra*). Upon removal from these chambers, the dogbones were immediately tested to minimize exposure to the lab environment. The data were collected in duplicate with samples placed at 10% strain at a rate of 120 mm/min and held under constant strain for 5 min. The light used for photocuring was a UV nail gel curing lamp with four 9 W bulbs (available online from ad hoc suppliers) with a peak emission at 360 nm and an intensity of 7.0 mW/cm<sup>2</sup>.

**Synthesis of thiol-ene networks.** The synthetic procedure was the same as previously described,<sup>43</sup> with samples mixed, sonicated, and cured with 360 nm UV light for 30 min using 1 wt% DMPA. All samples had a 75:25 ratio of DODT:PTMP, with the specific composition of the vinyl component being varied to substitute either free diol (99:1, 97:3, or 95:5 ratio of VPBE:APD molar equivalent of vinyl) or irreversible crosslinker (20:80, 15:85, 10:90, 3:97, 2:98, or 1:99 ratio of VPBE:TEGDVE molar equivalent of vinyl) for boronic ester diene while still maintaining a one-to-one ratio of thiol to vinyl groups (Table S1). Additionally, a sample with 20:79:1 ratio of VPBE:TEGDVE:APD was prepared, roughly equivalent to a combination of the 95:5 VPBE:APD and the 20:80 VPBE:TEGDVE. The same procedure was followed for

the reference material made with TEGDVE entirely in the place of VPBA. ATR-FTIR spectroscopy was used to monitor thiol conversion using the S–H absorption peak at 2590  $\text{cm}^{-1}$ . Thermal characterization of the final materials was performed by DSC.

**Water absorption studies.** Rectangular samples with either 95:5 VPBE:APD, 20:80 VPBE:TEGDVE, 15:85 VPBE:TEGDVE, 10:90 VPBE:TEGDVE, or 20:79:1 VPBE:TEGDVE:APD were weighed and then submerged in water for 14 days. Samples of each composition in duplicate were removed every 24 h, patted dry, and weighed before re-immersing.

**Humidity chamber preparation.** Constant humidity environments were prepared as previously reported.<sup>43,44</sup> Briefly, 23% and 85% humidity atmospheres were made by filling the bottom of sealed containers with saturated solutions of potassium acetate or potassium chloride, respectively. These salts were selected to minimize humidity variation within our typical laboratory temperature ranges, thereby optimizing the environments for use in controlled healing experiments.

**Network healing.** Three representatives of each network type (100:0, 99:1, 97:3, 95:5 VPBE:APD, 20:80, 15:85, 10:90 VPBE:TEGDVE, and combined 20:79:1 VPBE:TEGDVE:APD), were healed for 3 days under ambient conditions after dabbing the completely separated cut interfaces with water and reconnecting the two individual pieces along the freshly exposed interface. Samples with 95:5 VPBE:APD were also investigated for their ability to heal while heating (1.5 and 3 h at 70 °C), omitting the addition of water to the cut interface. For the samples containing irreversible TEGDVE crosslinks, a longer healing time (7 days) and up to 3 cycles of healing were also examined. Multiple healing cycles were carried out by repeatedly damaging and healing the material at the same location (as determined by cutting

near the “scar” of the previously damaged samples), with a 6 h drying time between cycles. After removal from the chambers, all samples exposed to humidity were vacuum dried for over 18 h with intermittent storage in a desiccator until their final weights were within 0.3% of their weights before exposure to humidity. All samples were characterized by tensile testing.

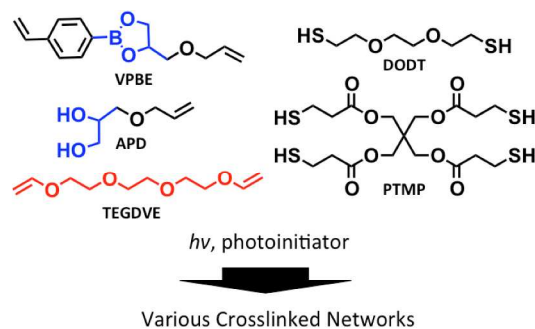


**Figure 2.** Synthesis of boronic ester network materials via photoinitiated thiol-ene curing.

## Results and Discussion

We previously demonstrated that bulk macroscopic healing could be achieved in low  $T_g$  networks capable of boronic ester exchange.<sup>43</sup> While efficient healing was possible, rapid exchange of the dynamic crosslinks also led to creep over extended times. To provide insight into the relationship between relaxation behavior and healing efficiency, we decided to consider two variables that would allow tuning of the dynamic behavior such that rapid and efficient healing could be achieved in a system that demonstrates less stress relaxation. By incorporating free diol functionality within a network crosslinked via boronic esters, crosslink exchange can be achieved by transesterification, thereby providing an alternative mechanism for dynamic behavior. On the other hand, to minimize the potentially detrimental effects of stress relaxation and creep, we also investigated the effect of incorporating irreversible crosslinks within boronic ester-containing materials (Figure 1).

### Networks with Boronic Esters and Free Diols

Boronic ester-crosslinked networks with various concentrations of free diol were made through thiol-ene chemistry.<sup>43</sup> These networks were fully cured as determined by ATR-FTIR spectroscopy via the absence of the thiol peak at  $2590\text{ cm}^{-1}$ . Varying amounts of free diol were used to prepare networks with different ratios of boronic esters to free diols: 99:1, 97:3, and 95:5 VPBE:APD. All compositions resulted in glass transition temperatures below room temperature, which led to sufficient molecular mobility to heal at ambient temperature (Table S2).

Since the presence of water has a significant influence on the rate of hydrolytic self-healing as well as the predominant healing mechanism when hydrolysis and transesterification are occurring simultaneously, the dynamic behavior of these materials was evaluated as a function of the humidity of the surrounding environment. However, beforehand, samples were also completely immersed in water to investigate their structural integrity. Even the samples with the highest concentration of free diol present in the network were stable, with only a slight increase in weight ( $\sim 5\%$ ) being observed over the course of 13 days as a result of a small amount of water absorption (Figure S1). All networks, regardless of free diol content, gradually became opaque over the course of the first day while submerged in water, suggesting that their hydrophobicity led to a collapsed skin layer forming on the surface of the samples, which likely limited infiltration of water (and the hydrolysis that would have resulted). However, the presence of free diol did seem to enhance chain mobility and resulted in samples that underwent slight macroscopic shape change from a thin rectangular shape to a more spherical form when submerged in water. This shape change occurred relatively quickly (12 h) after submersion and was not observed for the samples that contained no free diol. It should also be noted that while incorporation of the monovinyl free diol inevitably affects the overall macromolecular structure

by serving as a chain stopper during curing (*i.e.*, creating network defects), we reasoned that the resulting network-bound diol groups best represented the diol moieties formed by either hydrolysis or transesterification in boronic ester crosslinks.

The observed shape change during water exposure, as well as observations of creep even while stored in a dry environment, suggested the importance of more thoroughly investigating the effect of free diol content and the role of hydrolysis on the dynamic nature of these materials. Stress relaxation experiments were conducted to provide insight into the extent of crosslink exchange and the propensity for creep. Samples were conditioned in chambers of varying humidity before being immediately characterized for stress relaxation under tension. The characteristic relaxation time ( $\tau$ ) is defined below via a modified Maxwell model as the time required for the stress ( $\sigma$ ) to reach 37% ( $1/e$ ) of its original value ( $\sigma_0$ ) after accounting for the stress that the sample cannot physically relax ( $\sigma_{\text{plateau}}$ ) due to any permanent (*i.e.*, non-dynamic) network structure. Therefore, this value can be calculated as  $\tau = (1/e)(\sigma_0 - \sigma_{\text{plateau}})$  to facilitate direct comparison of the relaxation rate of various networks even though different compositions are capable of relaxing to various degrees because of their structure. Generally speaking, there appeared to be a significant increase in network mobility (*i.e.*, lower  $\tau$ ) for samples exposed to higher humidity environments or containing increasing concentrations of free diol. For example, when stress relaxation was investigated after conditioning the networks in dry atmospheres, where boronic ester hydrolysis should be minimal and the crosslink density of all samples could be assumed to be similar (Figure 3a), increasing the free diol content resulted in more rapid network relaxation. For example, at 0% humidity the relaxation time dropped from near 100 s down to 25 s for samples with 3 and 5% free diol, respectively. Although perhaps some of this change could be attributed to a higher concentration of network defects arising from

incorporation of the free diol, it is anticipated that the higher content of free diol also plays a key role in accelerating diol-boronic ester exchange (Table S3), which is consistent with free diol leading to accelerated bond exchange due to transesterification. At 23% humidity (Figure 3b), increasing free diol content (99:1, 97:3, and 95:5 VPBE:APD) even more significantly reduced relaxation times (107, 92, 41, and 7.3 s, respectively). At 85% humidity (Figure 3c), hydrolysis appears to be the dominant mechanism of crosslink exchange, with all compositions demonstrating relaxation times of approximately 1-2 s. These results suggest that both increased concentration of free diol and increased humidity led to accelerated crosslink exchange in boronic ester-containing materials. At relatively low humidities, the rate of exchange is strongly correlated with the concentration of free diol, as crosslink cleavage occurs primarily via transesterification. On the other hand, at higher humidities crosslink cleavage occurs mainly via hydrolysis, leading to a minimal effect of free diol concentration on the rate of stress relaxation. Given this, we demonstrated that networks containing 95:5 VPBE:APD with the most free diol could be reshaped after prolonged exposure to water (i.e., after immersion or exposure to high humidity environments) (Figure 3d), suggesting that these materials may have utility for applications that require recycling or reprocessability.<sup>45</sup>

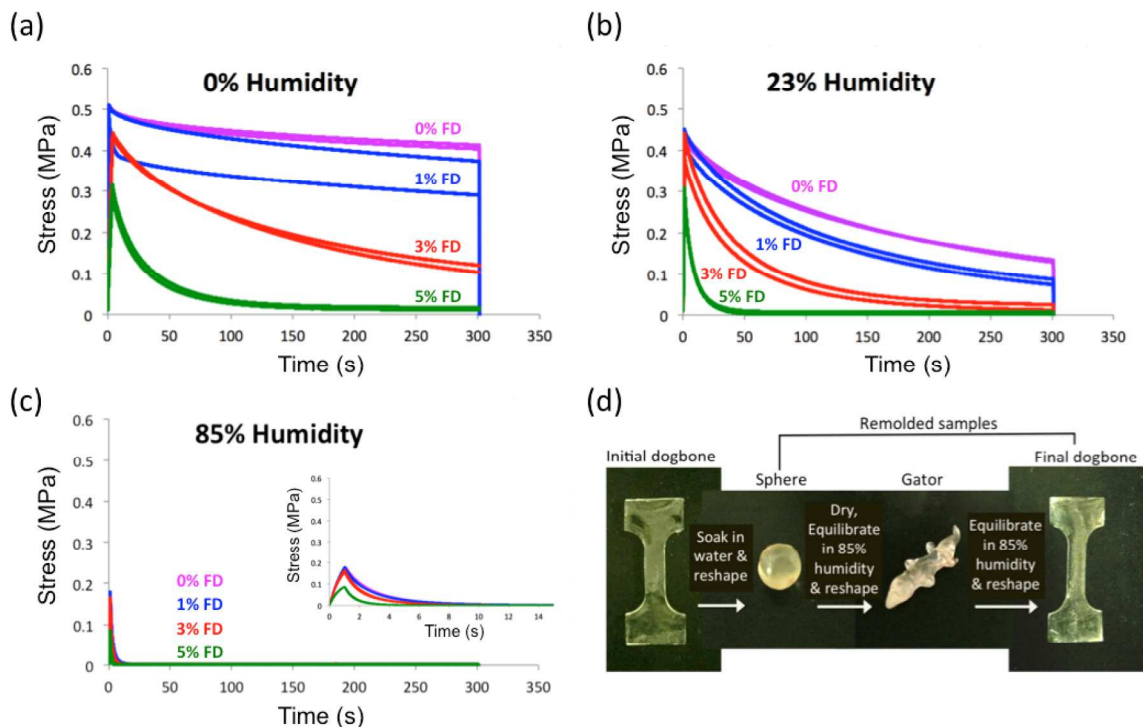


**Figure 3.** Stress relaxation of 99:1, 97:3, and 95:5 VPBE:APD free diol networks after exposure to (a) 0%, (b) 23%, and (c) 85% humidity. (d) Qualitative demonstration of 95:5 VPBE:APD free diol network remolding after immersion in water and exposure to 85% humidity.

Given the apparent exchange reactions occurring in both humid and dry environments during the stress relaxation experiments, healing in both environments was expected for networks containing free diol, unlike networks comprised purely of boronic esters.<sup>43</sup> To examine this, samples with and without free diol were exposed to humidity over time to determine whether they were capable of hydrolytic self-healing (i.e., hydrolysis and re-esterification). The materials were then subjected to tensile testing (Figure 4a and 4b). Exposure of damaged free diol-containing networks to high humidity resulted in healing similar to that observed with 100% boronic ester networks, with high healing efficiencies of 95% from peak stress. Healing was also investigated after the samples were exposed to dry environments. While networks without free

diol demonstrated no healing,<sup>43</sup> which is to be expected given that bond hydrolysis and re-esterification are predicted to be slow under these conditions,<sup>43</sup> networks containing 95:5 VPBE:APD free diol samples did demonstrate a modest degree of healing, with efficiencies of 45% from peak stress and 18% from strain at break being observed after 3 h at 70 °C. These results suggest that transesterification between free diols and boronic esters leads to crosslink exchange and healing even in the absence of water, a result that is consistent with the stress relaxation results observed for these networks at 0% humidity (Figure 4c and 4d). The relatively low healing efficiency likely results from the slow rate of exchange between diols and boronic esters.<sup>25</sup> These results also suggest that diol-boronic ester exchange plays a larger role during stress relaxation than potential network defects.

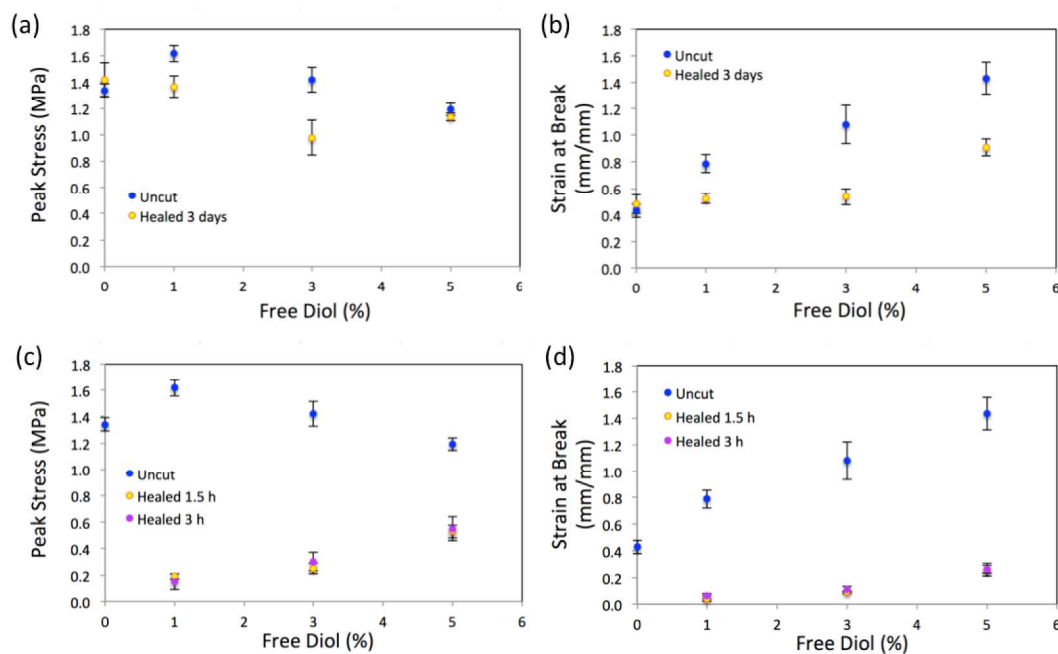


**Figure 4.** Evaluation of healing by tensile testing after exposure to humid environments (85% humidity for 3 days) (a and b) and after exposure to dry conditions (under vacuum and heating at 70 °C) (c and d).

### **Networks with Permanent Crosslinks and Boronic Esters**

While networks crosslinked via dynamic bonds can be healed, reprocessed, and responsive to certain environmental cues, a potential complication arises on a sufficiently long time scale when the material is under stress by tension, compression, bending, or gravity. In these cases, dynamic bond exchange can also lead to frequency-dependent rheological behavior, such as creep or plastic deformation. One solution to minimize the effects of creep or stress relaxation is to imbue the networks with a small fraction of irreversible crosslinks that impart structural integrity. We decided to evaluate the effect of including permanent crosslinks within our boronic ester materials, with particular attention being paid to the fraction of irreversible crosslinks that could be included without significantly compromising the benefits of the dynamic organoboron bonds.

TEGDVE was included during curing of dithiol, tetrathiol, and boronic ester diene to create networks that included both dynamic boronic esters and irreversible crosslinks. Quantitative curing was observed by observing the disappearance of the S-H absorbance at  $2590\text{ cm}^{-1}$  during FTIR spectroscopy, and all networks had glass transition temperatures below room temperature (Table S2). Because free diol was not intentionally incorporated in these networks, it was envisioned that healing would rely on hydrolysis and re-esterification of boronic esters. As compared to the materials previously considered, complete immersion of the samples in water led to an initial increase in mass due to water absorption followed by a gradual weight loss over time (Figure 5a). The reduction in mass after prolonged exposure to water is likely the result of a small amount of degradation by hydrolysis due to the increased hydrophilicity of the samples that resulted from incorporation of the relatively polar permanent crosslinker. This idea is further

supported by the fact that the networks containing increasing amounts of TEGDVE became less opaque when submerged in water.

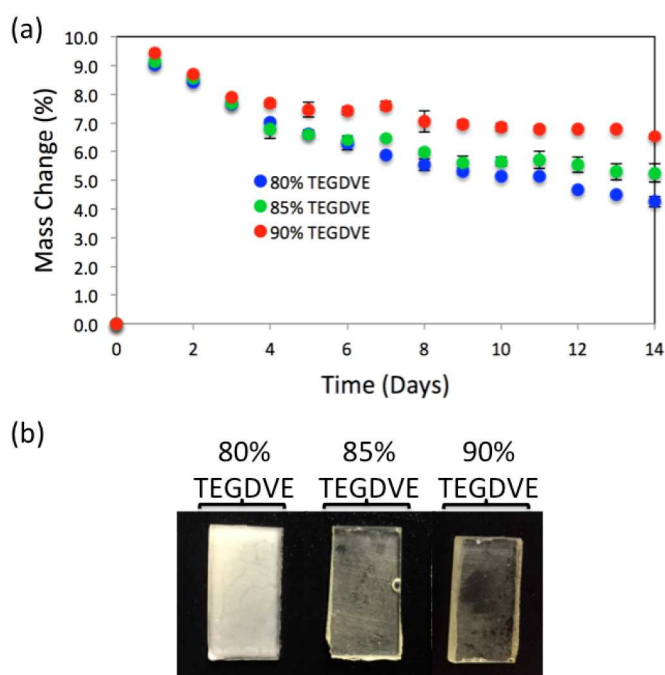


**Figure 5.** (a) Change in mass over time for networks containing 20:80, 15:85, and 10:90 VPBE:TEGDVE (i.e., permanent crosslinks) submerged in water and (b) images of the samples after exposure in water for 2 days.

Stress relaxation experiments were carried out for samples with various concentrations of permanent crosslinks that were equilibrated beforehand at 0, 23, or 85% humidity. As shown in Figure 6a, the networks that were aged in the lowest humidity environments and that contained the highest incorporation of TEGDVE demonstrated behavior that was most similar to covalently crosslinked networks. As the concentration of boronic ester was increased and the number of permanent crosslinks was decreased, the maximum stress at the start of the experiment increased

and a gradual decrease in the slope was apparent with time. This increase in stress, attributed to “catching” that occurs as the dynamic bonds reform and increase the maximum force needed for strain, is to be expected and has been previously observed in dynamic covalent networks.<sup>46</sup> By the same reasoning, this increased dynamic behavior associated with the increasing concentration of boronic ester also leads to a greater magnitude of relaxation. This is also true for samples equilibrated in the absence of moisture, because even atmospheric water present during testing could cause slight shifts in equilibrium, leading to a gradual relaxation and a lower plateau region that corresponds to a decrease in network crosslink density.

All samples pre-equilibrated in a dry environment had relaxation times greater than 100 s (Table S3), suggesting very slow bond exchange consistent with minimal effects of hydrolysis and re-esterification in the absence of water. Networks exposed to 23% humidity (Figure 6b) relaxed faster, as expected, with the plateau level of the curves decreasing with increasing concentration of the hydrolytically labile boronic ester bonds. Following the same trend of increased humidity leading to faster bond exchange, networks exposed to the highest humidity of 85% (Figure 6c) demonstrated the fastest relaxation times. For all networks exposed to humid environments, an increased content of permanent crosslinks led to reduced and slower stress relaxation.

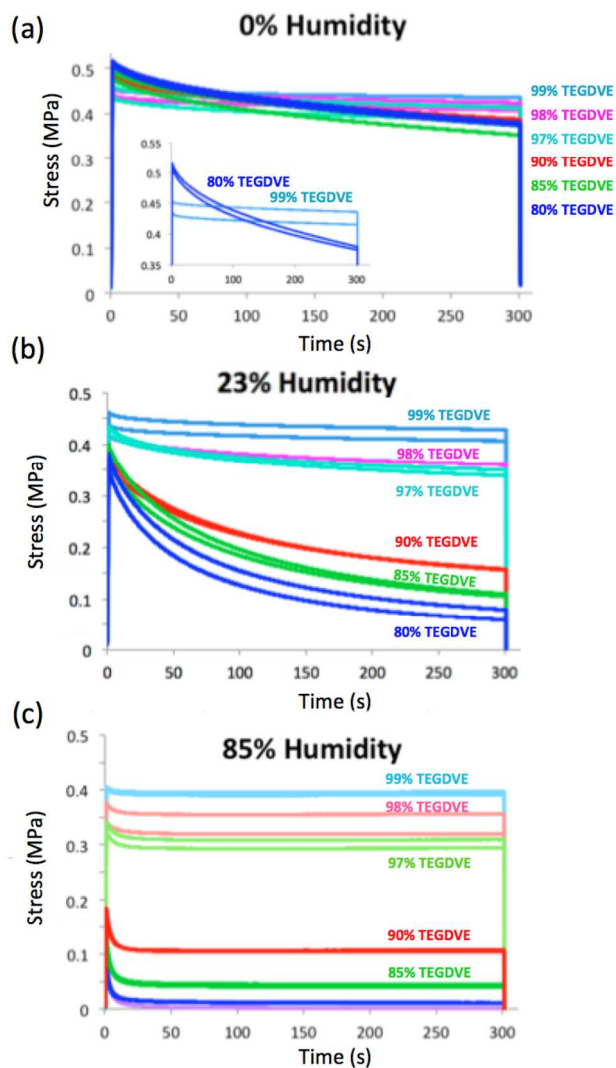


**Figure 6.** Stress relaxation data for 20:80, 15:85, and 10:90 VPBE:TEGDVE permanent crosslinker networks after exposure to (a) 0%, (b) 23%, and (c) 85% humidity.

Tensile testing was used to elucidate the effect of incorporating permanent crosslinks on healing efficiency (Figure 7a and 7b). Healed samples demonstrated maximum stress (86%) and strain at break (90%) values that were within error of the virgin samples for the networks in which 80% of the crosslinks were permanent (i.e., 20% boronic ester crosslinks, 20:80 VPBE:TEGDVE). The incorporation of permanent crosslinks in dynamic-covalent networks

leads to an increased potential for irreversible bond cleavage during damage and thus a lower possibility of full recovery after healing. Therefore, repeat healing experiments were undertaken in which samples were repeatedly cut and healed at the same location. The sample with 80% of the crosslinks being permanent, 20:80 VPBE:TEGDVE, were selected for testing due to their excellent healing and moderate stress relaxation at low humidity. After three healing cycles, both peak stress and strain at break were within error of the values obtained for the virgin materials prior to damage (Figure 7c and 7d). These results suggest that healing can be efficient even when the majority of crosslinks present in the network are non-dynamic.

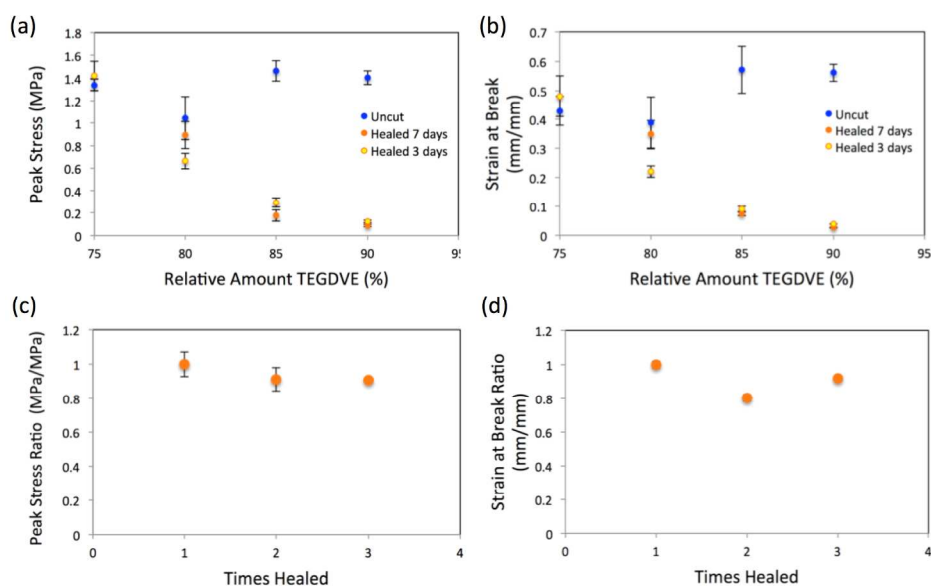


**Figure 7.** Self-healing of boronic ester networks as evaluated by tensile testing.

(a) Maximum stress and (b) elongation at break as a function of the relative amount of permanent crosslinker (TEGDVE) and healing time. (c) Maximum stress and (d) elongation at break of boronic ester network materials with 20:80 VPBE:TEGDVE after multiple cycles of damage and repair

### Combined Free Diol and Permanent Crosslinker Networks

Given the separate benefits of incorporating free diols for faster healing and permanent crosslinks for reduced stress relaxation and creep, we prepared networks that contained both components in a single system. By including both types of crosslinker, it was anticipated that the less desirable aspects of each system could be mitigated (i.e., creep in the free diol networks and low healing efficiency in the permanently crosslinked networks). To test this hypothesis, a network (20:79:1 VPBE:TEGDVE:APD) that contained roughly 5% free diol (95:5 VPBE:APD) and 80% irreversible diene (20:80 VPBE:TEGDVE) was selected, as these concentrations, when incorporated individually, showed optimal behaviors. These networks were observed to undergo a mass loss of approximately 6% over nine days (Figure S2). The presence of free diol and TEGDVE led to a network that was more hydrophilic than those considered earlier, which may have facilitated hydrolysis of the exterior of the material. However, no further mass loss was observed after 9 days, as the networks became opaque over time and their shapes remained fixed, suggesting that the materials are relatively stable to hydrolysis over extended periods.

The stress relaxation behavior of these materials showed that the mechanical behavior most closely resembled that of the networks that contained permanent crosslinks alone (i.e., without free diol) (Figure 8, Table S3). As the substitution of 80% irreversible diene for boronic ester diene affects a greater fraction of the network than incorporation of the relatively small amount of 5% free diol, this trend observed in relaxation behavior is expected. These results indicate that the propensity of these hybrid materials to undergo creep is relatively minimal.

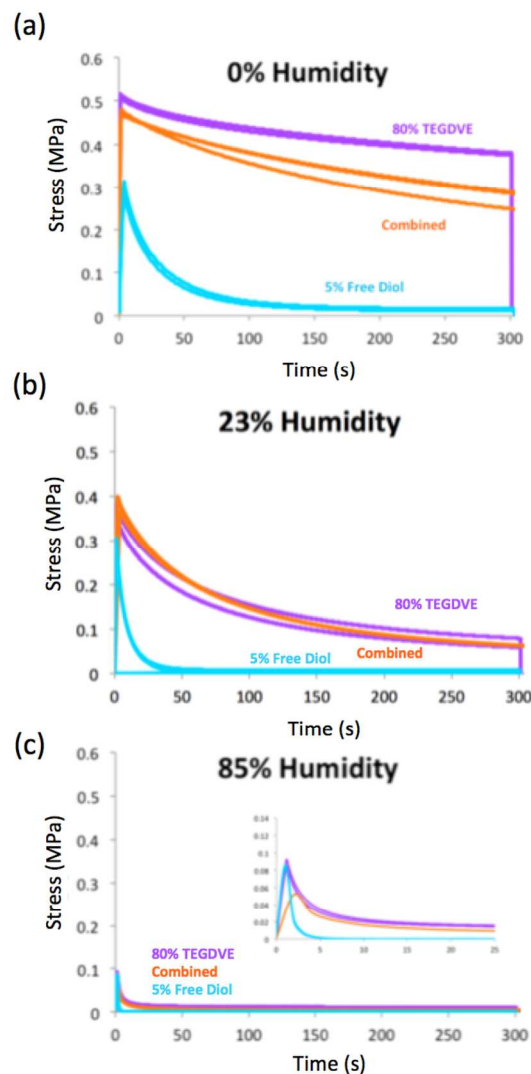


**Figure 8.** Stress relaxation curves run in duplicate of samples containing free diol (95:0:5 VPBE:TEGDVE:APD), permanent crosslinker (20:80:0 VPBE:TEGDVE:APD), and both in combination (20:79:1 VPBE:TEGDVE:APD) after exposure to (a) 0%, (b) 23%, and (c) 85% humidity.

Finally, while the shape and structural integrity in response to external forces was much improved, an evaluation of the effect of combining both approaches on healing efficiency was also carried out. Healing efficiency was determined by tensile experiments, comparing the peak

stress and strain at break of the virgin and healed materials. The extent of healing was measured after three days, as samples with only free diol showed good healing efficiency in this time frame, while the samples with permanent crosslinker required longer for similar healing. The hybrid networks demonstrated healing behavior that was intermediate to those of the networks with only free diol or permanent crosslinks alone (Figure 9). These results provide important insight and guidance into the role of reversible (associative and dissociative) and irreversible crosslinks into healable materials.

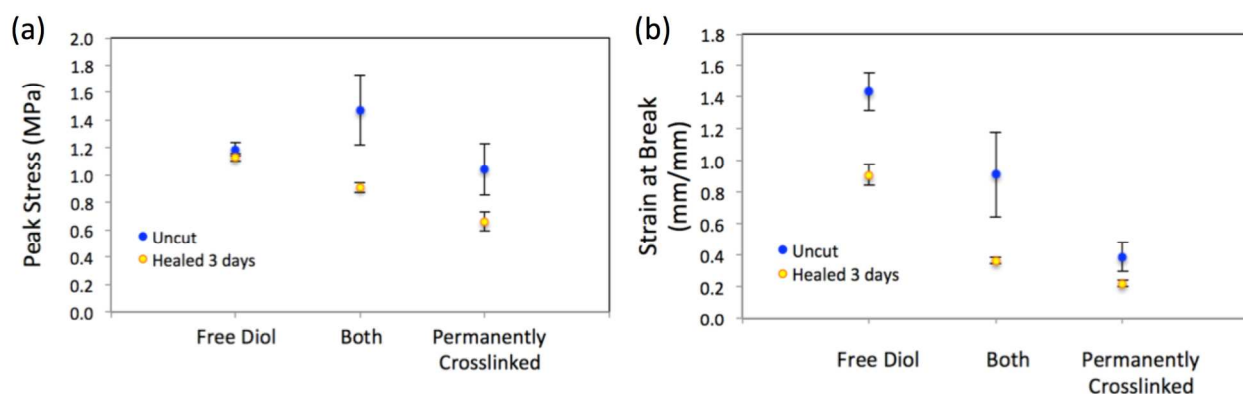


**Figure 9.** Self-healing of boronic ester network materials as evaluated by tensile testing after 3 days of healing. (a) Peak stress and (b) strain at break recovery measured by tensile testing for samples containing 95:0:5 VPBE:TEGDVE:APD, 20:80:0 VPBE:TEGDVE:APD, or 20:79:1 VPBE:TEGDVE:APD.

## Conclusion

These experiments demonstrate that polymeric networks crosslinked via dynamic-covalent boronic esters can be modified to improve healing efficiency and to reduce stress relaxation and creep by the incorporation of free diol or permanent crosslinks, respectively. While materials crosslinked exclusively via boronic esters undergo exchange by hydrolysis and re-esterification, or potentially by boronic ester metathesis, including free diols within the

networks allows an additional method of bond exchange to occur by transesterification. Including this associative mechanism of exchange allows for samples with higher healing efficiencies at the expense of faster stress relaxation and creep. On the other hand, stress relaxation and creep can be moderated by the incorporation of permanent crosslinks that lend increased structural integrity, albeit with a loss of healing efficiency. In all cases, the mechanical and healing behavior of the materials was dependent on the humidity of the environment to which the networks were exposed and the healing time. Arguably, the materials that demonstrated the best balance of rapid bond exchange to promote healing and static crosslinks to provide structural integrity were those that contained both free diols and permanent crosslinks. These results may provide insight into the design of dynamic-covalent materials that rely on other examples of reversible covalent bonds.

### **Associated Content**

Supporting Information Available:

Additional DSC, water absorption, and relaxation time results. This material is available free of charge via the Internet at <http://pubs.acs.org>.

### **Acknowledgements**

This material is based upon work supported by the National Science Foundation (DMR-1606410 and DMR-1410223). J.J.C. and D.J.D. thank the DOD for a Science Mathematics and Research for Transformation Fellowship.

### **References**

- (1) Scott, T. F.; Schneider, A. D.; Cook, W. D.; Bowman, C. N. *Science* **2005**, *308*, 1615-1617.
- (2) Roy, N.; Bruchmann, B.; Lehn, J.-M. *Chem. Soc. Rev.* **2015**, *44*, 3786-3807.
- (3) Amamoto, Y.; Otsuka, H.; Takahara, A.; Matyjaszewski, K. *Adv. Mater.* **2012**, 3975-3980.
- (4) Otsuka, H. *Polym. J.* **2013**, *45*, 879-891.
- (5) Garcia, S. J. *Eur. Polym. J.* **2014**, *53*, 118-125.
- (6) Rowan, S. J.; Cantrill, S. J.; Cousins, G. R. L.; Sanders, J. K. M.; Stoddart, J. F. *Angew. Chem. Int. Ed.* **2002**, *41*, 898-952.
- (7) Denissen, W.; Winne, J. M.; Du Prez, F. E. *Chem. Sci.* **2016**, *7*, 30-38.
- (8) Stukalin, E. B.; Cai, L.-H.; Kumar, N. A.; Leibler, L.; Rubinstein, M. *Macromolecules* **2013**, *46*, 7525-7541.
- (9) Yang, H.; Yu, K.; Mu, X.; Shi, X.; Wei, Y.; Guo, Y.; Qi, H. J. *Soft Matter* **2015**, *11*, 6305-6317.
- (10) Capelot, M.; Unterlass, M. M.; Tournilhac, F.; Leibler, L. *ACS Macro Lett.* **2012**, *1*, 789-792.
- (11) Capelot, M.; Montarnal, D.; Tournilhac, F.; Leibler, L. *J. Am. Chem. Soc.* **2012**, *134*, 7664-7667.
- (12) Montarnal, D.; Capelot, M.; Tournilhac, F.; Leibler, L. *Science* **2011**, *334*, 965-968.
- (13) Lu, Y.-X.; Tournilhac, F.; Leibler, L.; Guan, Z. *J. Am. Chem. Soc.* **2012**, *134*, 8424-8427.
- (14) Pepels, M.; Filot, I. A. W.; Klumperman, B.; Goossens, H. *Polym. Chem.* **2013**, *4*, 4955-4965.
- (15) Brutman, J. P.; Delgado, P. A.; Hillmyer, M. A. *ACS Macro Lett.* **2014**, *3*, 607-610.
- (16) Rekondo, A.; Martin, R.; Ruiz de Luzuriaga, A.; Cabañero, G.; Grande, H. J.; Odriozola, I. *Mater. Horiz.* **2014**, *1*, 237-240.
- (17) Denissen, W.; Rivero, G.; Nicolaÿ, R.; Leibler, L.; Winne, J. M.; Du Prez, F. E. *Adv. Funct. Mater.* **2015**, *25*, 2451-2457.
- (18) Obadia, M. M.; Mudraboyina, B. P.; Serghei, A.; Montarnal, D.; Drockenmuller, E. *J. Am. Chem. Soc.* **2015**, *137*, 6078-6083.
- (19) Fortman, D. J.; Brutman, J. P.; Cramer, C. J.; Hillmyer, M. A.; Dichtel, W. R. *J. Am. Chem. Soc.* **2015**, *137*, 14019-14022.
- (20) Romano, F.; Sciortino, F. *Phys. Rev. Lett.* **2015**, *114*, 078104-078105.
- (21) Imbernon, L.; Oikonomou, E. K.; Norvez, S.; Leibler, L. *Polym. Chem.* **2015**, *6*, 4271-4278.
- (22) Röttger, M.; Domenech, T.; van der Weegen, R.; Breuillac, A.; Nicolaÿ, R.; Leibler, L. *Science* **2017**, *356*, 62-65.
- (23) Hall, D. G. In *Boronic acids: preparation and applications in organic synthesis and medicine*; Wiley-VCH: Weinheim, 2005, p ACS Applied Materials & Interfaces.
- (24) Lennox, A. J. J.; Lloyd-Jones, G. C. *Chem. Soc. Rev.* **2014**, *43*, 412-443.
- (25) Cromwell, O. R.; Chung, J.; Guan, Z. *J. Am. Chem. Soc.* **2015**, *137*, 6492-6495.
- (26) Zhang, B.; Digby, Z. A.; Flum, J. A.; Foster, E. M.; Sparks, J. L.; Konkolewicz, D. *Polym. Chem.* **2015**, *6*, 7368-7372.
- (27) Fox, C. H.; ter Hurne, G. M.; Wojtecki, R. J.; Jones, G. O.; Horn, H. W.; Meijer, E. W.; Frank, C. W.; Hedrick, J. L.; a, J. M. G. i. *Nat. Commun.* **2015**, *6*, 1-8.
- (28) Iyer, B. V. S.; Salib, I. G.; Yashin, V. V.; Kowalewski, T.; Matyjaszewski, K.; Balazs, A. C. *Soft Matter* **2013**, *9*, 109-121.

- (29) Sordo, F.; Mougner, S.-J.; Loureiro, N.; Tournilhac, F.; Michaud, V. *Macromolecules* **2015**, *48*, 4394-4402.
- (30) Döhler, D.; Peterlik, H.; Binder, W. H. *Polymer* **2015**, *69*, 264-273.
- (31) Nicolaÿ, R.; Kamada, J.; Van Wassen, A.; Matyjaszewski, K. *Macromolecules* **2010**, *43*, 4355-4361.
- (32) Mukherjee, S.; Bapat, A. P.; Hill, M. R.; Sumerlin, B. S. *Polym. Chem.* **2014**, *5*, 6923-6931.
- (33) Bapat, A. P.; Ray, J. G.; Savin, D. A.; Sumerlin, B. S. *Macromolecules* **2013**, *46*, 2188-2198.
- (34) Bapat, A. P.; Roy, D.; Ray, J. G.; Savin, D. A.; Sumerlin, B. S. *J. Am. Chem. Soc.* **2011**, *133*, 19832-19838.
- (35) Bapat, A. P.; Ray, J. G.; Savin, D. A.; Hoff, E. A.; Patton, D. L.; Sumerlin, B. S. *Polym. Chem.* **2012**, *3*, 3112-3120.
- (36) De, P.; Gondi, S. R.; Roy, D.; Sumerlin, B. S. *Macromolecules* **2009**, *42*, 5614-5621.
- (37) Figg, C. A.; Simula, A.; Gebre, K. A.; Tucker, B. S.; Haddleton, D. M.; Sumerlin, B. S. *Chem. Sci.* **2015**, *6*, 1230-1236.
- (38) Roy, D.; Sumerlin, B. S. *Macromol. Rapid Commun.* **2014**, *35*, 174-179.
- (39) Cambre, J. N.; Roy, D.; Sumerlin, B. S. *J. Polym. Sci., Part A: Polym. Chem.* **2012**, *50*, 3373-3382.
- (40) Roy, D.; Cambre, J. N.; Sumerlin, B. S. *Chem. Commun.* **2009**, 2106-2108.
- (41) Mukherjee, S.; Brooks, W. L. A.; Dai, Y.; Sumerlin, B. S. *Polym. Chem.* **2016**, *7*, 1971-1978.
- (42) Deng, C. C.; Brooks, W. L. A.; Abboud, K. A.; Sumerlin, B. S. *ACS Macro Lett.* **2015**, 220-224.
- (43) Cash, J. J.; Kubo, T.; Bapat, A. P.; Sumerlin, B. S. *Macromolecules* **2015**, *48*, 2098-2106.
- (44) Greenspan, L. *J. Res. NBS A Phys. Chem.* **1977**, *81A*, 89.
- (45) Taynton, P.; Yu, K.; Shoemaker, R.; Jin, Y.; Qi, H. J.; Zhang, W. *Adv. Mater.* **2014**, *26*, 3938-3942.
- (46) Salib, I. G.; Kolmakov, G. V.; Gnegy, C. N.; Matyjaszewski, K.; Balazs, A. C. *Langmuir* **2011**, *27*, 3991-4003.